

Supporting Information for  
**Structural reconstruction of germanosilicate framework by  
controlled hydrogen reduction**

Yue Ma,<sup>a</sup> Hao Xu,<sup>a</sup> Xue Liu,<sup>a</sup> Mingming Peng,<sup>a</sup> Wenting Mao,<sup>b</sup> Lu Han,<sup>b,c\*</sup>  
Jingang Jiang<sup>a\*</sup> and Peng Wu<sup>a\*</sup>

*<sup>a</sup>Shanghai Key Laboratory of Green Chemistry and Chemical Processes, School of Chemistry and Molecular Engineering, East China Normal University, North Zhongshan Rd. 3663, Shanghai, 200062, China*

*<sup>b</sup>State Key Laboratory of Metal Matrix Composites, School of Chemistry and Chemical Engineering, Shanghai Jiao Tong University, Shanghai, 800 Dongchuan Road, 200240, China*

*<sup>c</sup>School of Chemical Science and Engineering, Tongji University, 1239 Siping Road, Shanghai, 200092, China*

## **Experimental Section**

### ***Material preparation***

According to the literatures [1, 2], UTL-type germanosilicate was hydrothermally synthesized with (6R, 10S)-6, 10-dimethyl-5-azoniaspiro [4. 5] decane hydroxide as organic structure-directing agent (OSDA). The gel with a molar composition 1.0 SiO<sub>2</sub>: 0.5 GeO<sub>2</sub>: 0.375 OSDA(OH) : 37.5 H<sub>2</sub>O was crystallized in a Teflon-lined autoclave at 170 °C for 7 days under rotation (10 rpm). The as-made product was collected by filtration, washing with deionized water, and drying at 100 °C overnight. It was further calcined in air at 550 °C for 6 h, burning off the included organic species and obtaining the parent UTL sample in calcined form.

### ***Gas-solid reduction process***

The solid-gas reduction with hydrogen was conducted on the parent UTL germanosilicate to induce top-down structural transformations. 0.2 g of UTL sample in calcined form, placed in a quartz tube reactor (i.d. 1.6 cm), was pretreated at 25 °C for 20 min in a dry N<sub>2</sub> stream (30 mL min<sup>-1</sup>). Then, the N<sub>2</sub> stream was switch to H<sub>2</sub> stream (30 mL min<sup>-1</sup>) and the reactor was brought to a desired treatment temperature (400 - 680 °C) with a rate of 5 °C min<sup>-1</sup>. The reduction treatment under H<sub>2</sub> atmosphere was maintained for different periods of time (1 - 9 h). After cooling to room temperature in N<sub>2</sub>, the reduced sample was collected for subsequent treatments, denoted as *Rn* (*n* indicated the treatment time).

### ***Purification process***

To obtain pure-phase zeolites, the reduced Ge metal crystals or clusters were removed by a successive calcination and water-washing process. The reduced *Rn* sample was calcined in air at 710 °C for 6 h, to completely oxidize the Ge metal crystals or clusters into germanium oxide. The calcined sample was denoted as *Rn-ox*. Thereafter, the calcined sample *Rn-ox* was dispersed in deionized water with a solid-to-liquid ratio of 1: 50. This suspension was heated to 90 °C under stirring at 500 rpm for 1 h. The product was then collected by filtration and washing with deionized water, followed by drying at 80 °C overnight and further calcination in air at 550 °C for 6 h, denoted as *Rn-ox-H<sub>2</sub>O*.

### **Characterization methods**

Temperature-programmed-reduction of H<sub>2</sub> (H<sub>2</sub>-TPR) was carried on the parent UTL gemernosilicate on the Autochem 2920 automatic chemical adsorption instrument equipped with a thermal conductivity detector. The pristine UTL sample (0.1 g), placed in a stainless tube, was pretreated at 500 °C for 1 hour with He (50 mL min<sup>-1</sup>) to remove any impurities and moisture. Then, the sample was cooled to 50 °C followed by purging with 10% H<sub>2</sub>-Ar flow (50 mL min<sup>-1</sup>) for 30 min. After the baseline was stable, the sample was heated to 1000 °C at a constant rate of 10 °C min<sup>-1</sup>.

<sup>1</sup>, during which the H<sub>2</sub> consumption curve (TPR profile) was recorded.

Powder X-ray diffraction (PXRD) was employed to check the structure and crystallinity of the zeolites. The patterns were collected on a Rigaku Ultima IV diffractometer using Cu K $\alpha$  radiation at 35 kV and 25 mA with a step width of 0.02° in the 2 $\theta$  range of 5° - 30°.

Nitrogen gas adsorption measurements were carried out at -196 °C on a BEL-MAX gas/vapor adsorption instrument. The samples were evacuated at 300 °C for at least 6 h before measurements. The specific surface areas were calculated by the Brunauer-Emmett-Teller (BET) method. The *t*-plot method was used to determine micropore volume.

The pore size distribution was calculated with Horvath-Kawazoe method based on the data collected by Ar adsorption at 87 K on a Micromeritics ASAP 2020 instrument.

The IR spectra in the framework vibration region were collected on a Nicolet Nexus 670 FT-IR spectrometer in absorbance mode at a spectral resolution of 2 cm<sup>-1</sup> using KBr technique (2 wt% wafer).

The <sup>29</sup>Si MAS NMR spectra were measured on a VARIAN VNMRS 400WB NMR spectrometer at a frequency of 79.43 MHz using one pulse method, a spinning rate of 3 kHz, a recycling delay of 60 s. The chemical shift was referred to the standard of Q<sub>8</sub>M<sub>8</sub> [(CH<sub>3</sub>)<sub>3</sub>SiO]<sub>8</sub>SiO<sub>12</sub>.

Thermogravimetry (TG) analyses were carried out on a Mettler TGA/SDTA 851e instrument with a ramping rate of 10 °C min<sup>-1</sup> in 50 mL min<sup>-1</sup> mixed flowing gas of N<sub>2</sub> and H<sub>2</sub>.

The Ge content was determined by inductively coupled plasma emission spectrometry (ICP) on a Thermo IRIS Intrepid II XSP atomic emission spectrometer after dissolving the samples in HF solution or aqua regia.

Scanning electron microscopy (SEM) images were measured on A Hitachi S-4800 microscope coupled with an energy dispersive X-ray detector (EDX) to determine the crystal morphology and element content.

The three-dimensional electron diffraction tomography (3D- EDT) data collected on a JEOL JEM-2100 microscope that was equipped with a LaB<sub>6</sub> gun operated at 200 kV

(Cs 1.0 mm, point resolution of 2.3 Å). A TENGRA CCD camera (2304 × 2304 pixels with a 2:1 fiber-optical taper and an effective pixel size of 18 μm<sup>2</sup>) was used for digital recording of the diffraction pattern. The collected dataset was processed using the EDT Process software.

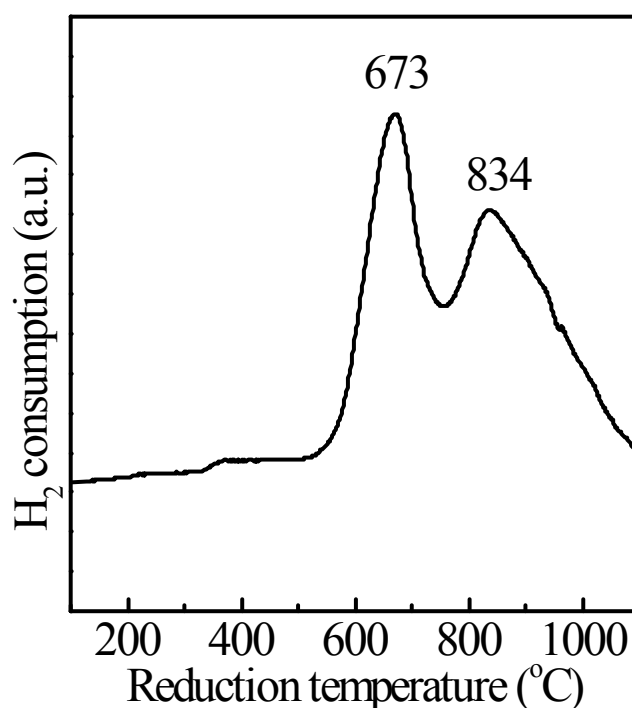


**Figure S1.** H<sub>2</sub>-TPR profile of the parent UTL germanosilicate.

*Two significant H<sub>2</sub> consumption signals at 673 and 834 °C were observed from the H<sub>2</sub>-TPR profile of UTL germanosilicate. The former was ascribed to the reduction of Ge atoms located in the vulnerable interlayer D4R units while the latter was probably attributed to the reduction of Ge atoms embeded in the Si-rich layers.*

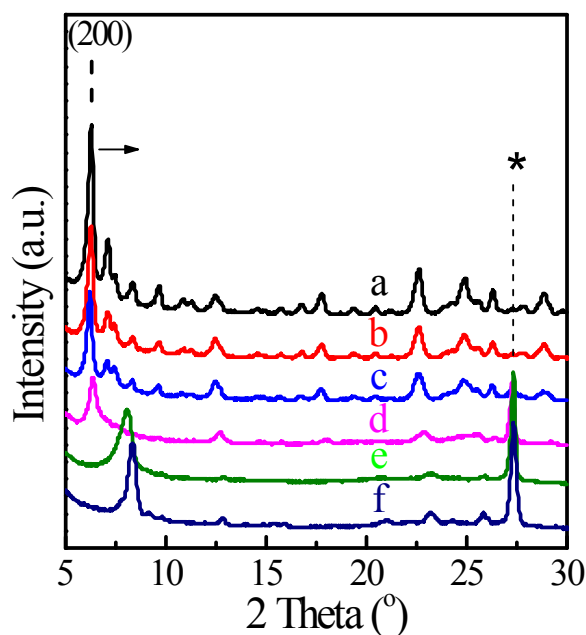


**Figure S2.** PXRD patterns of the parent UTL germanosilicate (a), after reduced by H<sub>2</sub> at 400 °C (b), 500 °C (c), 600 °C (d), 650 °C (e), 680 °C (f) for 6 h, respectively. The asterisk indicates the Ge metal-related diffraction.

*The 200 reflection peak shifted to higher angles upon raising the reduction temperature. The PXRD patterns of the resultant samples displayed an obvious structural transformation when the H<sub>2</sub> reduction was performed at a high temperature of 680 °C, which was assessed by an apparent shift of the 200 reflection from the original 2θ angle of 6.2° to 8.3° after reduction, accompanied by the emergence of a sharp diffraction located at 2θ = 27.2° attributed to the cubic phase Ge metal with a typical diamond structure (Ge-I) [3]. This result indicated that the germanosilicate structure was readily reorganized by extracting the Ge species out the framework via solid-gas H<sub>2</sub> reduction.*

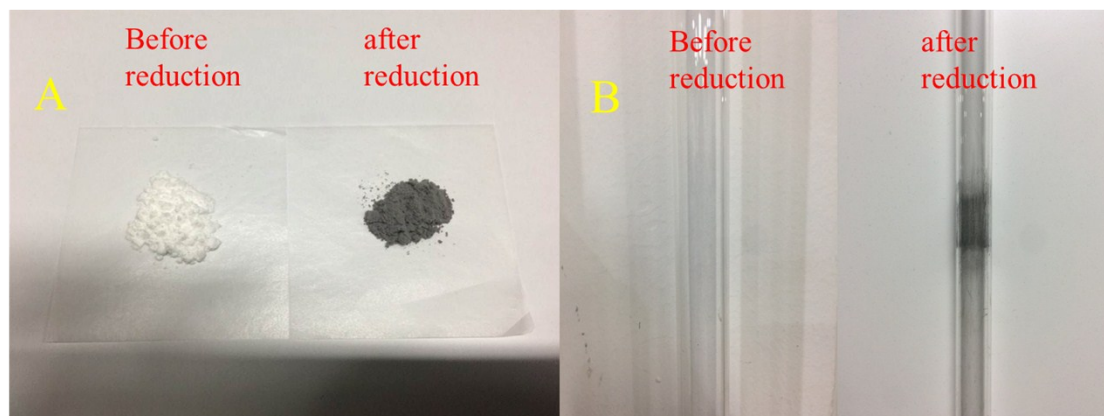


**Figure S3.** The images of the parent UTL germanosilicate (A) and quartz tube reactor (B) before and after H<sub>2</sub> reduction.

*The white powder of UTL germanosilicate turned to dark gray after H<sub>2</sub> reduction at 680 °C, probably due to the emergence of Ge metal crystals. Meanwhile, the inner wall of the quartz tube reactor showed the same color due to the sublimated metal germanium.*

**Table S1.** Physicochemical properties of UTL and its derived samples.

Sample	$S_{\text{BET}}^{\text{a}}$ ( $\text{m}^2 \text{g}^{-1}$ )	$V_{\text{micro}}^{\text{a}}$ ( $\text{cm}^3 \text{g}^{-1}$ )	Si/Ge ratio <sup>b</sup>
Parent UTL	449	0.17	4.7
R1	215	0.08	5.0
R5	264	0.09	5.2
R9	248	0.09	6.1
R1-ox-H <sub>2</sub> O	321	0.12	27.3
R5-ox-H <sub>2</sub> O	295	0.10	30.6
R9-ox-H <sub>2</sub> O	260	0.09	38.2

<sup>a</sup> Specific surface area and micropore volume given by N<sub>2</sub> adsorption at 77 K.

<sup>b</sup> Determined by ICP analysis.

*The resultant samples after H<sub>2</sub> reduction showed dramatically lower specific surface area and micropore volume than the parent UTL. On one hand, the decreased interlayer space revealed by the PXRD patterns (Figure 1) induced lower surface area and micropore volume. On the other hand, the nonporous and relative heavy Ge metal also contributed to the decreased surface area and micropore volume. Interestingly, the sample R1 reduced for a short time led to the lowest surface area and the smallest micropore volume, while longer reduction time leads to enhance the surface area and micropore volume (R5 and R9). The reduced small Ge metal clusters or nanoparticles may block the channels within a short reduction time, while with prolonging reduction time at harsh temperatures, the Ge particles would grow in size and migrate out of the pores.*

*After removing the Ge crystals via calcination and water-washing process, the bulk Si/Ge ratios increased to 27.3 - 38.2 for the R1-ox-H<sub>2</sub>O, R5-ox-H<sub>2</sub>O and R9-ox-H<sub>2</sub>O samples, and the specific surface area and micropore volume also increased obviously as the pores were opened and the nonporous Ge crystals was extensively removed.*

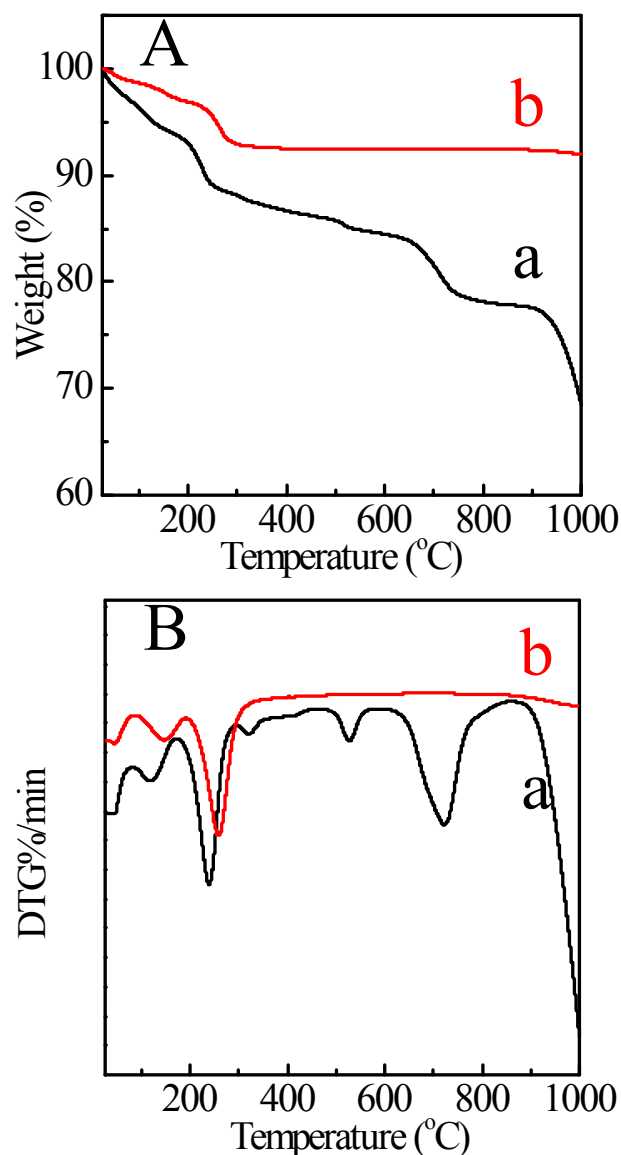


**Figure S4.** Thermogravimetric analysis (A) and differential thermal gravity (B) of the calcined UTL germanosilicate under  $H_2$  (a) and  $N_2$  (b) atmospheres.

*The TG analysis and DTG of calcined germanosilicate under both  $N_2$  and  $H_2$  atmospheres were performed and different TG and DTG curves were observed. More specifically, there was almost the only two weight-loss platform ascribed to the removal of physical adsorbed water located on the outer surface and inside the aperture under  $N_2$  atmosphere, while more weight-loss steps appeared in  $H_2$  atmosphere. Additionally, the total weight-loss in  $H_2$  (30 wt. %) was larger than that in  $N_2$  (8 wt. %), due to the removal of oxygen and escape of fractional reduced germanium.*

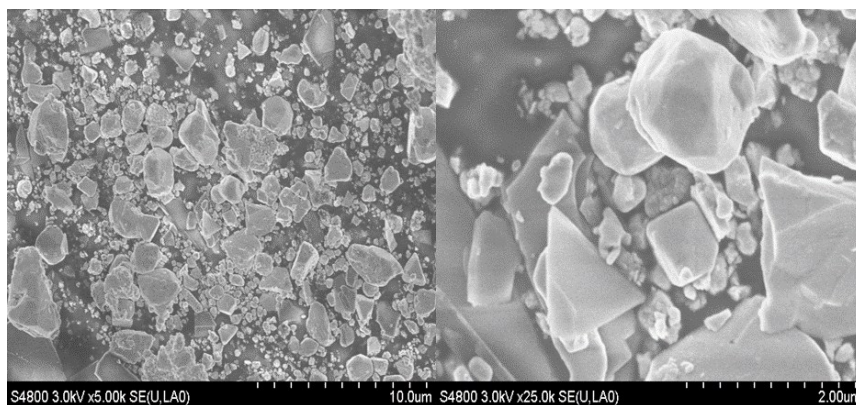


**Figure S5.** SEM images of the dark gray product attached to the inner wall of the quartz tube reactor after reduction.

*Both Ge metal and UTL zeolite were observed on the inner wall of the quartz tube reactor after reduction.*

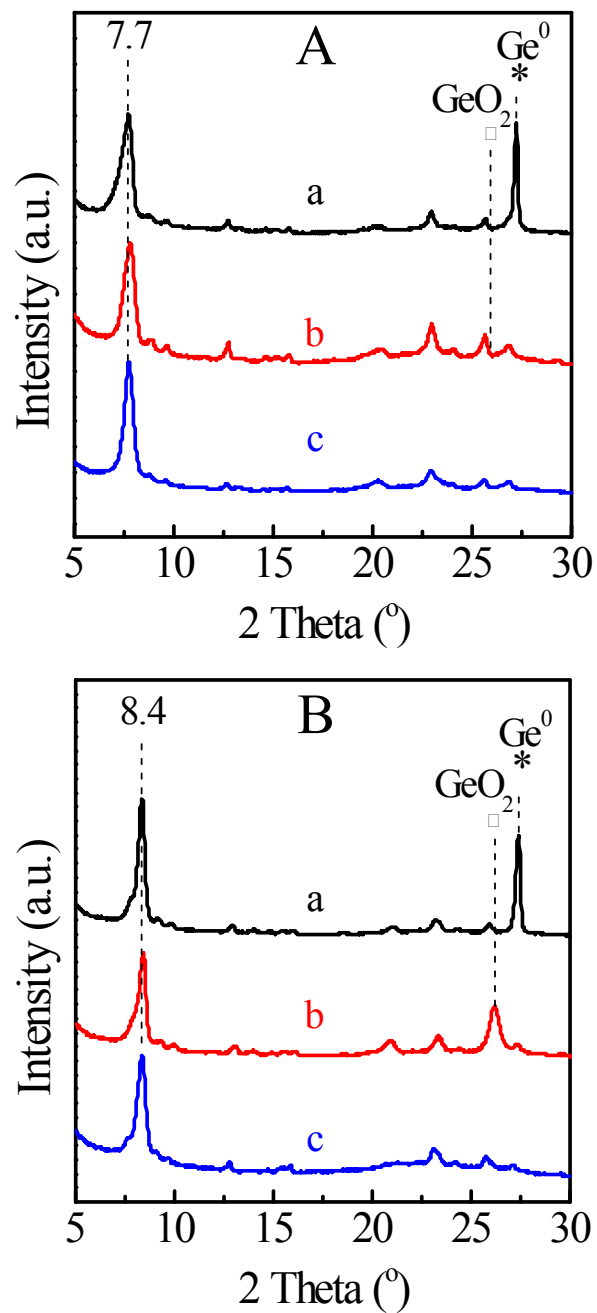


**Figure S6.** (A) PXR D pattern of R1 (a), R1-ox (b), and R1-ox-H<sub>2</sub>O (c). (B) PXR D pattern of R9 (a), R9-ox (b), and R9-ox-H<sub>2</sub>O (c). The asterisk and triangle indicate the diffraction peaks attributed to Ge metal and GeO<sub>2</sub>, respectively.

*For the sample R9, the UTL layer-related 200 reflection transferred to  $2\theta = 8.4^\circ$  (Figure S6B, a) with losing Ge atoms from the framework. Correspondingly, a sharp*

*diffraction peak at  $2\theta=27.2^\circ$  emerged (Figure S6B, a), which was attributed to the cubic phase Ge metal (JCPDS Card No. 04-0545, Fd-3m (227)). The calcination in air made it disappear in the sample R9-ox and a new one developed at  $2\theta = 26.0^\circ$  (Figure S6B, b), assigned to  $\text{GeO}_2$ . The germanium oxide was then removed after water-washing, corresponding to the disappearance of the peak at  $2\theta = 26.0^\circ$  (Figure S6B, c). The Si/Ge ratio was increased to 38.2 for R9-ox- $\text{H}_2\text{O}$  (Table S1).*

*The pure material of R1-ox- $\text{H}_2\text{O}$  was obtained eventually by the same treatment. It is worth noting that the calcination in air made the diffraction peak ( $2\theta = 27.2^\circ$ ) disappear but the new one at  $2\theta = 26.0^\circ$  (Figure S6A, b) assigned to  $\text{GeO}_2$  not obvious, which may be due to the fewer particles and high dispersity of germanium oxide.*

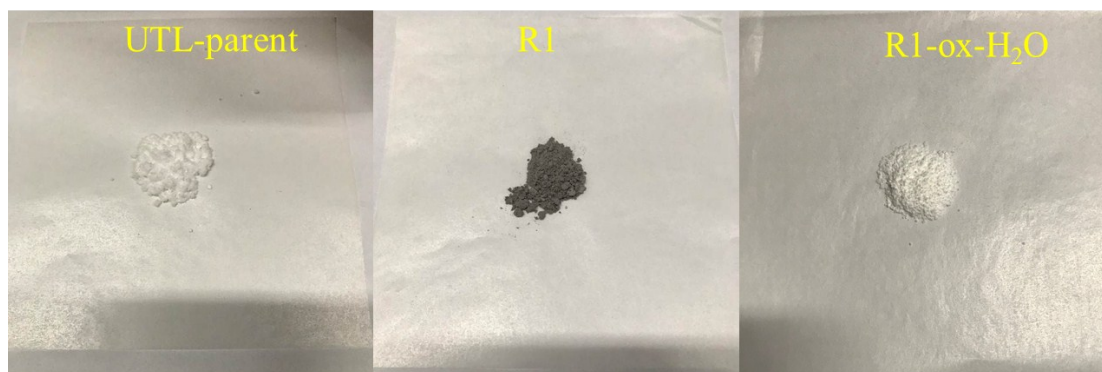


**Figure S7.** The image of parent UTL germanosilicate, R1 and R1-ox-H<sub>2</sub>O samples.

*The color of UTL changed from white to dark gray after hydrogen reduction at 680 °C, because the framework Ge ions were partially reduced to the metallic Ge crystals.*

*The white color was restored after the Ge crystals were oxidized by calcination in air.*

*The white color was still maintained after further water washing (not shown).*

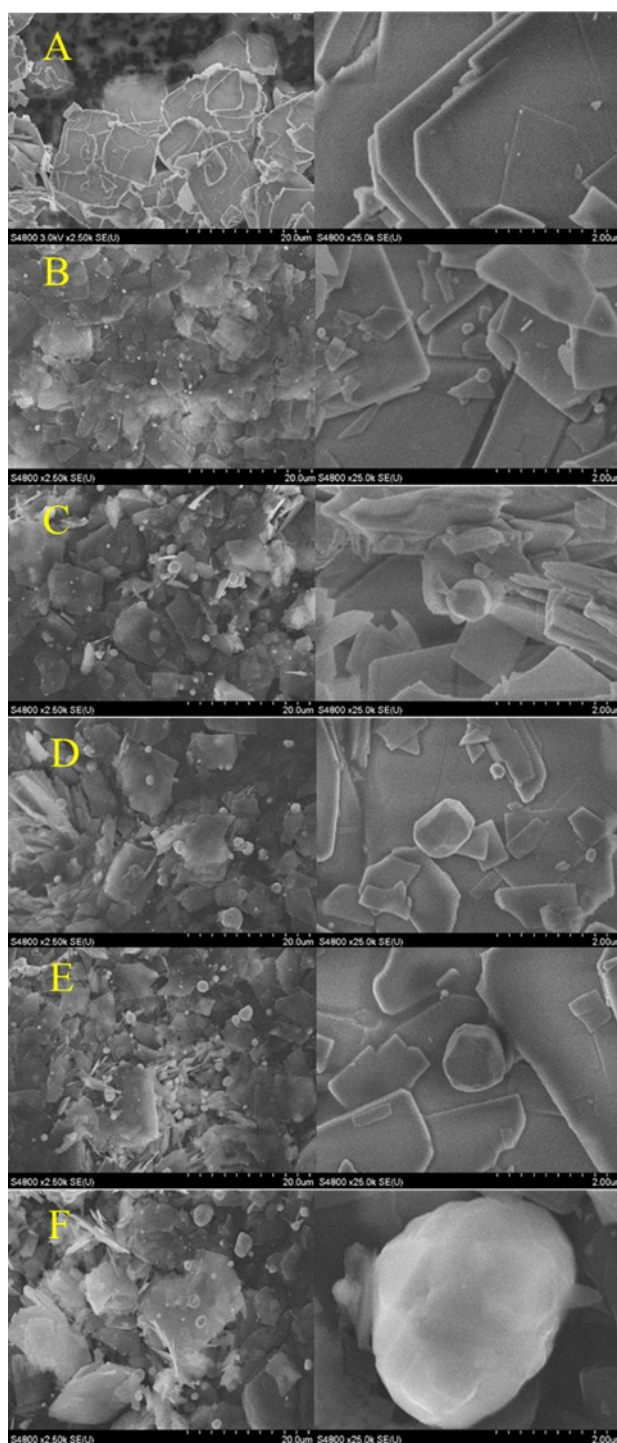


**Figure S8.** SEM images of the parent UTL germanosilicate (A), after reduced by  $H_2$  at 680 °C for 1 h (B), 3 h (C), 5 h (D), 7 h (E), and 9 h (F), respectively.

*The parent UTL germanosilicate was composed of the platelet-like crystals free of impurity. With prolonging the time of hydrogen reduction, the Ge particles emerged gradually and their size grew from nanometer to micrometer scale.*

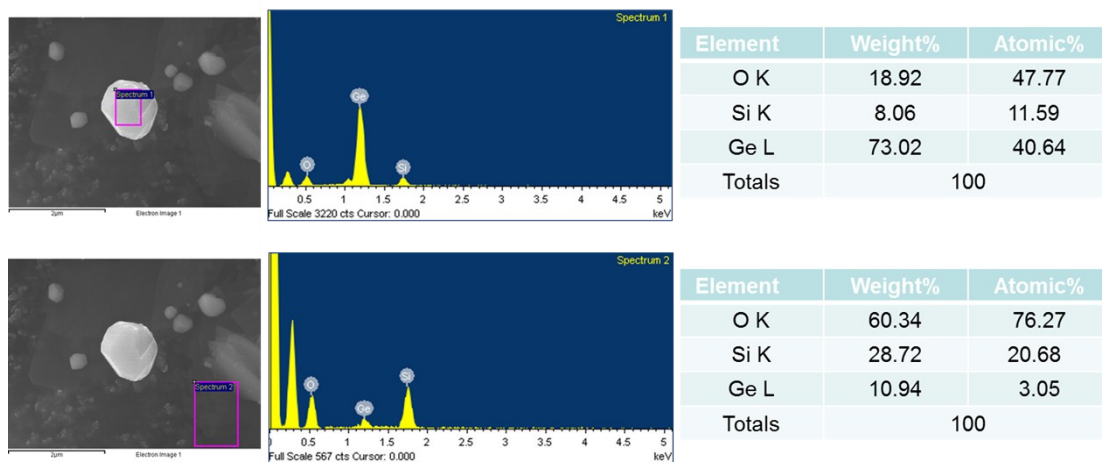


**Figure S9.** Energy dispersive X-ray (EDX) analysis of the sample after reduction.

*The results showed that the round-shaped particles newly formed upon hydrogen reduction contained mainly Ge, indicating the formation of Ge metal crystals.*

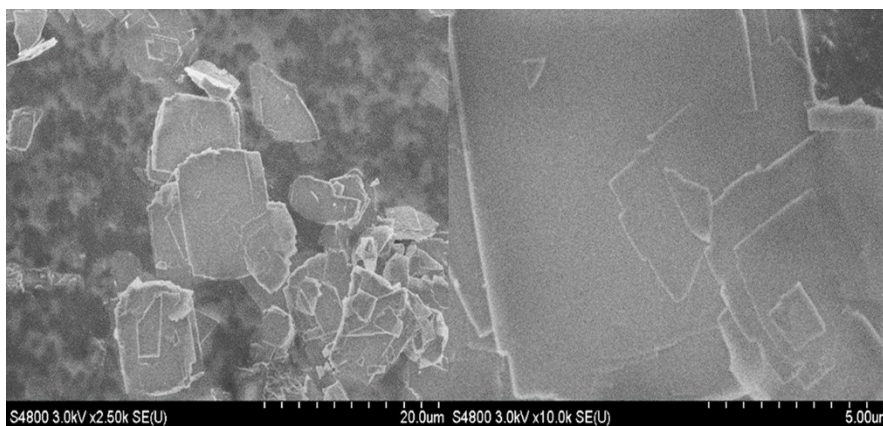


**Figure S10.** SEM images of R1-OX-H<sub>2</sub>O.

*R1-OX-H<sub>2</sub>O was free of the reduced metal germanium, indicating the Ge metal could be removed by the combination of calcination and water washing process.*

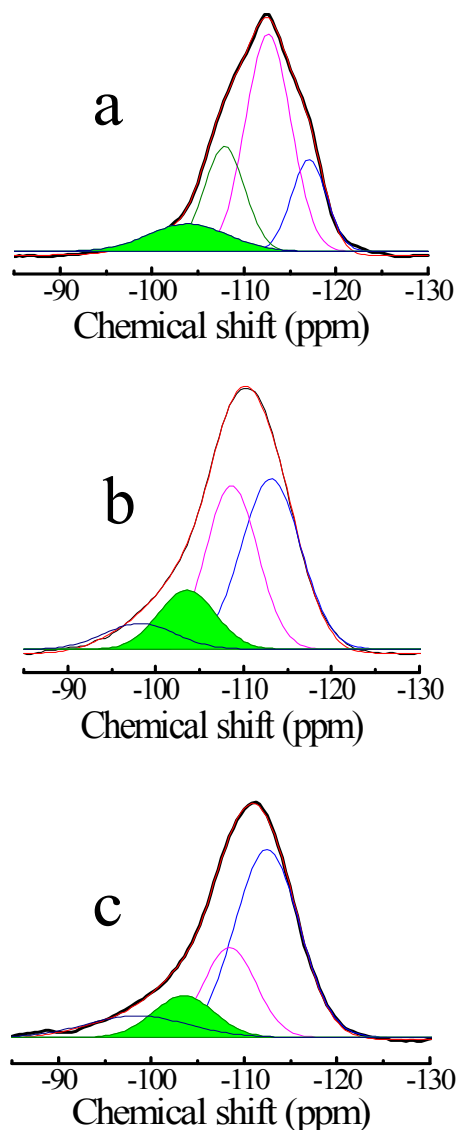


**Figure S11.**  $^{29}\text{Si}$  MAS NMR spectra of the parent UTL germanosilicate (a), R1-ox- $\text{H}_2\text{O}$  (b) and R9-ox- $\text{H}_2\text{O}$  (c). The deconvoluted lines marked in green show the components assigned to the  $\text{Q}^3$  groups.

*The parent UTL sample showed a resonance at  $\delta = -107.8$  ppm which is assigned to the Si atoms linked with germanium [4]. The signal almost completely disappeared in R1-ox- $\text{H}_2\text{O}$  and R9-ox- $\text{H}_2\text{O}$ , implying a deep depletion of Ge. Instead, R1-ox- $\text{H}_2\text{O}$  and R9-ox- $\text{H}_2\text{O}$  possessed more  $\text{Q}^3$  and  $\text{Q}^2$  groups, meaning more defects were created as a result of germanium departure from the frameworks during reduction process.*

**Table S2.**  $^{29}\text{Si}$  MAS NMR chemical shifts and peak area of the calcined UTL germanosilicate, R1-ox-H<sub>2</sub>O and R9-ox-H<sub>2</sub>O samples.

Sample	Peak	$\delta$ (ppm)	Area (%)	Attribution
Parent UTL	1	-117.09	16.58	Q <sup>4</sup>
	2	-112.65	50.43	
	3	-107.80	21.80	Si-Ge
	4	-103.76	11.19	Si-Ge or Q <sup>3</sup>
R1-ox-H <sub>2</sub> O	1	-113.26	42.56	Q <sup>4</sup>
	2	-108.82	35.54	
	3	-103.57	14.18	Q <sup>3</sup>
	4	-98.32	7.72	Q <sup>2</sup>
R9-ox-H <sub>2</sub> O	1	-112.46	56.07	Q <sup>4</sup>
	2	-108.42	21.88	
	3	-103.57	11.81	Q <sup>3</sup>
	4	-98.32	10.24	Q <sup>2</sup>

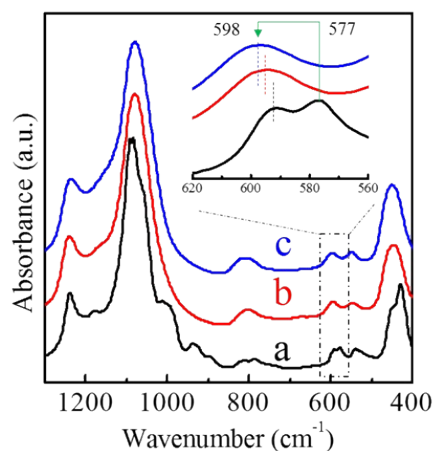


**Figure S12.** IR spectra in the framework vibration region of the parent UTL germanosilicate (a), R1-ox-H<sub>2</sub>O (b) and R9-ox-H<sub>2</sub>O (c). Insets showed the enlarged region for D4R vibration.

The band around 1000 cm<sup>-1</sup>, attributed to the asymmetric stretching vibration of Si-O-Ge in the framework [5], nearly disappeared for sample R1-ox-H<sub>2</sub>O and R9-ox-H<sub>2</sub>O as a result of extensive Ge removal. On the other hand, the band around 592 cm<sup>-1</sup> related to the vibration of D4R units in parent-UTL disappeared corresponding to the removal of D4R units [6] and the band around 577 cm<sup>-1</sup> still existed but with a blue shift after reduction treatment, attributed to the decrease of framework Ge content [7].

This should be replaced by "3D-EDT"

**Table S3.** RED: experimental parameters and crystallographic data of R1-OX-H<sub>2</sub>O

Comment [W□]: This should be replaced by "3D-EDT"

and R9-OX-H<sub>2</sub>O.

Samples	R1-OX-H <sub>2</sub> O	R9-OX-H <sub>2</sub> O
Tilt range (°)	-57.5 to 47.7	-47.69 to 46.28
Tilt step (°)	0.2	0.1
Wave length (Å)	0.0251	0.0251
No. of frames	570	1020
space group	C2/m	C2/m
Unit cell parameters	a=23.52, b=13.70, c=12.28, $\alpha=89.50$ , $\beta=109.42$ , $\gamma=90.00$	a=22.60, b=13.57, c=12.01, $\alpha=89.6$ , $\beta=110.00$ , $\gamma=90.00$
Volume (Å <sup>3</sup> )	3731.63	4361.03
Resolution (Å)	0.86	1.10
Completeness (%)	16.0	27.5
No. of total reflections	9242	12878

**Notes and references**

- 1 A. Corma, M. J. Díaz-Cabañas, F. Rey, S. Nicolopoulos and K. Boulahya, *Chem. Commun.*, 2004, **10**, 1356.
- 2 J. L. Paillaud, B. Harbuzaru, J. Patarin and N. Bats, *Sci.*, 2004, **304**, 990.
- 3 L. A. Villaescusa and M. A. Camblor, *Chem. Mater.*, 2016, **28**, 7544.
- 4 A. Rojas and M. A. Camblor, *Angew. Chem. Int. Ed.*, 2012, **51**, 3854.
- 5 T. Blasco, A. Corma, M. J. Díaz-Cabañas, F. Rey, J. A. Vidal-Moya and C. M. Zicovich-Wilson, *J. Phys. Chem. B*, 2002, **106**, 2634.
- 6 A. J. M. de Man and R. A. van Santen, *Zeolites*, 1992, **12**, 269.
- 7 C. S. Blackwell, *J. Phys. Chem.*, 1979, **83**, 3251.